SCIENTIFIC REPORTS

OPEN

SUBJECT AREAS:
MICROFLUIDICS
MECHANICAL ENGINEERING

Received
3 July 2013

Accepted
15 November 2013

Published
19 December 2013

Correspondence and requests for materials should be addressed to K.H.K. (khkang@postech.ac.kr) or G.L. (limmems@postech.ac.kr)

Ion concentration polarization-based continuous separation device using electrical repulsion in the depletion region

Hyungkook Jeon[1], Horim Lee[1], Kwan Hyoung Kang[1] & Geunbae Lim[1,2]

[1]Department of Mechanical Engineering, Pohang University of Science and Technology (POSTECH), San 31, Hyoja-dong, Nam-Gu, Pohang, Gyeongbuk, 790-784, the Republic of Korea, [2]Division of Integrative Bioscience and Biotechnology, Pohang University of Science and Technology (POSTECH), San 31, Hyoja-dong, Nam-Gu, Pohang, Gyeongbuk, 790-784, the Republic of Korea.

We proposed a novel separation method, which is the first report using ion concentration polarization (ICP) to separate particles continuously. We analyzed the electrical forces that cause the repulsion of particles in the depletion region formed by ICP. Using the electrical repulsion, micro- and nano-sized particles were separated based on their electrophoretic mobilities. Because the separation of particles was performed using a strong electric field in the depletion region without the use of internal electrodes, it offers the advantages of simple, low-cost device fabrication and bubble-free operation compared with conventional continuous electrophoretic separation methods, such as miniaturizing free-flow electrophoresis (μ-FFE). This separation device is expected to be a useful tool for separating various biochemical samples, including cells, proteins, DNAs and even ions.

Electrophoresis is a common technique used in biochemistry to separate biomolecules such as proteins, peptides, DNAs and cells[1]. Various separation techniques based on electrophoresis have been developed to achieve high sensitivity, short separation times and high throughput[1]. Among separation techniques, miniaturizing free-flow electrophoresis (μ-FFE) has attracted attention over the last 50 years because it offers the advantages of continuous flow separation and microfluidics[1–4]. In μ-FFE, charged particles are injected into a thin carrier flow, and an electric field is applied perpendicular to the flow[4]. As the charged particles pass through the electric field, they are deflected from the flow at an angle determined by the flow velocity, electrophoretic mobility and electric field strength[4]. Therefore, it is possible to separate samples based on their electrophoretic mobility. The sample separation can be easily optimized by controlling the applied external electric field. Also, sample injection, separation, and collection can be achieved continuously because the direction of the separation is perpendicular to that of the bulk flow. Due to these inherent advantages of μ-FFE, the technique has been considered to be compatible for integration with other elements of micro total analysis systems (μ-TAS) and actively used to separate various samples, including proteins, enzymes, membrane particles, organelles and cells[4].

However, there are some problems to be solved due to the internal electrodes. Fundamentally, its fabrication process is complicated; multi-step etching and integration of electrodes with the device are generally involved[5–8]. The internal electrodes also cause bubble formation in the device, which is one of the most challenging issues with μ-FFE[9]. Bubbles within the separation channel disturb the separation process because they may distort both the fluidic stream and the electric field[1]. In the recent years, many technological approaches have been proposed to prevent the bubbles from entering into the separation channel. For example, some research groups fabricated open-type μ-FFE devices which had exposed electrodes to allow ventilation of the bubbles[5,9,10]. In closed-type μ-FFE device, membrane-like structures[6,7,11] and an insulting wall[12] have been used to isolate the separation channel from the electrodes. Although the various methods have greatly contributed to solve the bubble problem in μ-FFE, those methods unintentionally have limited the utilization of μ-FFE at the same time. Because of the complex device design and additional blocking structures between the separation channel and electrodes, the fabrication became more complicated and challenging. Additionally, the blocking structures caused the loss of electric field and interrupted the presence of a stable and continuous electric field, resulting in low efficiency and poor

performance[10]. To overcome the limitations of μ-FFE including the bubble problem and difficulty in fabrication, we propose a novel electrophoretic separation technique based on ion concentration polarization (ICP).

ICP is a fundamental transport phenomenon in which ion-depletion and ion-enrichment regions are generated under an external electric field applied across an ion perm-selective membrane[13–15]. Recently, ICP has been used in various applications such as sample concentrators[3,16–18], desalinator[19] and micro-mixers[20]. Most of them used electrical repulsion in the depletion region to concentrate or filter out samples. However, the mechanism of the repulsion has not yet been investigated in detail. In the depletion region, the electric field strength increases due to the low ionic concentration. Therefore, electrokinetic motions, such as electroosmosis and electrophoresis, are significantly amplified[21]. Furthermore, the rapid increase in electric field strength in the depletion region can induce nonuniformity of the electric field. Thus, the dielectrophoretic force, as well as the electrophoretic force, can be applied to particles in the depletion region[18].

In the present study, the electrical forces in the depletion region were analyzed according to applied voltage and the size and electrophoretic mobility of the particles. We demonstrated that the electrophoretic force was dominant for the repulsion of particles in the depletion region. By using the electrophoretic force, micro- and nano-sized particles were separated depending on their electrophoretic mobility. Because the electric field was applied using external electrodes, this new separation method offers very simple and low-cost fabrication and can be free from the bubble formation which is the critical problem of conventional continuous electrophoretic separation methods, such as μ-FFE.

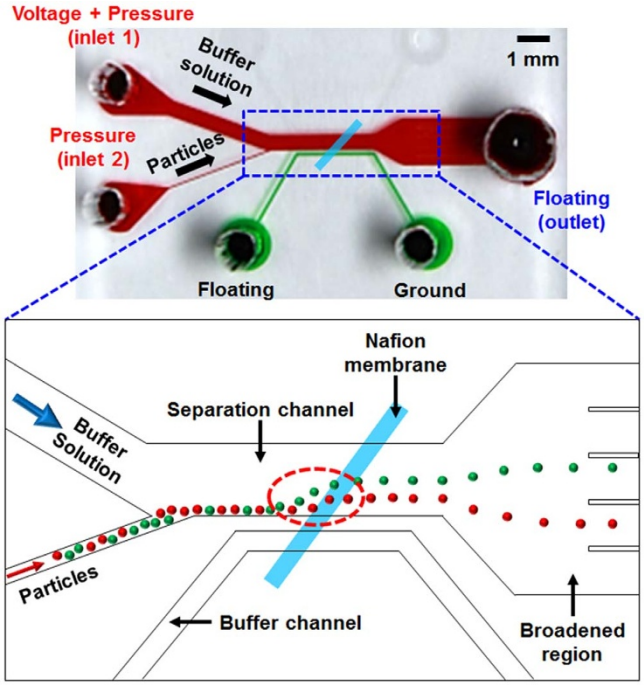

Figure 1 | Schematic diagram of the separation device and separation process. (Microchannel: polydimethylsiloxane (PDMS); nanojunction: Nafion membrane; microchannel height: 40 μm. Different colors represent particles having different properties; the red dotted circle denotes the ion-depletion region).

Results

Electrical repulsion of particles in depletion region. Figure 1 shows the layout of the ICP-based separation device and a schematic diagram of the separation process. To apply an electric field to the device, anode and cathode electrodes were connected to the metallic syringe tube of Inlet 1 and reservoir of the buffer channel, respectively. The electric field applied across the membrane induced an ion-depletion region (red circle in Figure 1) on the anodic side due to its strong cation selectivity[3]. A flow-focusing method[22] was used to drive the particles to the lower side wall of the separation channel, causing the particles to pass through the depletion region, where the electrical force was strong.

First, we demonstrated the effects of electrical force on the movement of particles passing through the depletion region. As shown in Figure 2a–c, the particle trajectories were shifted when moving over the membrane. Here, the shift is expressed as a repulsion distance, defined as the distance between the particle and the lower side wall after passing over the membrane. The repulsion distance is determined by competition between hydrodynamic drag and electrical forces. In the depletion region, an electrical repulsive force was applied to the particles, causing them to recede from the lower side wall. Particles moved a greater distance from the wall until the repulsive force became negligible compared with the hydrodynamic drag force. Therefore, the repulsion distance from the lower side wall increased with increasing electric field strength (Figure 2a–c). When the applied voltage was higher than a critical voltage (120 V under the conditions of Figure 2), particle motion was completely stopped by the repulsive force, and the particles were concentrated in front of the membrane (Figure 2d).

Theoretical analysis of electrical forces. We thought that three kinds of forces might be involved in particle movement in the depletion region: hydrodynamic drag, electrophoretic and dielectrophoretic forces. Because particles have negative electrophoretic mobilities, the electrophoretic force acts in the opposite direction of the electric field. The dielectrophoretic force is applied to the particles in the direction of decreasing electric field strength due to the lower polarizabilities of the particles compared with the buffer solution[23]. Therefore, both types of electrical forces can cause the particles to deviate from the fluid streamline (Figure 3).

For the Stokes regime (low Reynolds number regime), the inertial effect is negligible. Therefore,

$$\sum \mathbf{F} = \mathbf{F_H} + \mathbf{F_{EP}} + \mathbf{F_{DEP}} = 0, \quad (1)$$

where $\mathbf{F_H}$, $\mathbf{F_{EP}}$ and $\mathbf{F_{DEP}}$ denote hydrodynamic drag, electrophoretic and dielectrophoretic forces, respectively. For a spherical particle of radius a under a dc electric field $\mathbf{E}$, those three forces are expressed as[24]

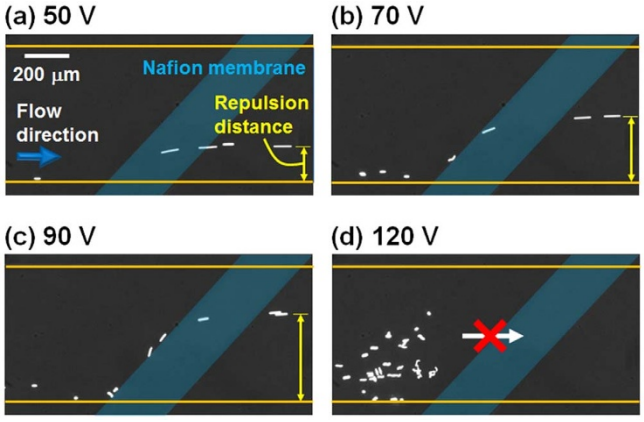

Figure 2 | Movement of 4.8-μm particles around the membrane depending on applied voltage; (a) 50 V, (b) 70 V, (c) 90 V, (d) 120 V (flow rate of Inlet 1: 1.0 μL/min; flow rate of Inlet 2: 50 nL/min; membrane thickness: 1.3 μm).

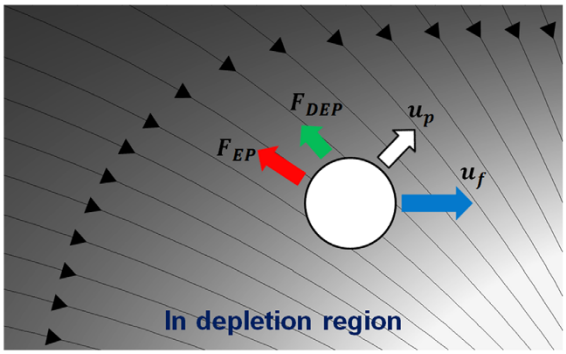

Figure 3 | Schematic diagram of the particle movement. A negatively charged spherical particle is exerted by hydrodynamic drag and electrical forces in the depletion region. The brightness indicates the magnitude of the electric field strength, E.

$$\mathbf{F_H} = -6\pi\mu a(\mathbf{u_p} - \mathbf{u_f}), \quad (2)$$

$$\mathbf{F_{EP}} = 6\pi\zeta_p\varepsilon_f a\mathbf{E}, \quad (3)$$

$$\mathbf{F_{DEP}} = -2\pi\varepsilon_f a^3\mathbf{E}\bullet\nabla\mathbf{E}, \quad (4)$$

where μ, ε_f and $\mathbf{u_f}$ represent the dynamic viscosity, electrical permittivity and velocity of the surrounding flow, and ζ_p and $\mathbf{u_p}$ are the dynamic viscosity and particle velocity, respectively.

We can substitute equations (2)–(4) into equation (1) and rearrange the equation to solve for $\mathbf{u_p}$. Then, the particle velocity can be obtained,

$$\mathbf{u_p} = \mathbf{u_f} - \mu_p\mathbf{E} - \frac{\varepsilon_f a^2}{3\mu}(\mathbf{E}\bullet\nabla)\mathbf{E}, \quad (5)$$

where $\mu_p = -\varepsilon_f\zeta_p/\mu$ represents the electrophoretic mobility of the particle.

On the right side of equation (5), the second term represents the electrophoretic velocity, which is proportional to only the electrophoretic mobility and independent of the radius of the particle, and the third term indicates the dielectrophoretic velocity, which is proportional to the square of the radius.

Experimental comparison of dielectrophoretic and electrophoretic effects. To identify which electrical force dominated the lateral deviation of the particle trajectory, we compared the repulsion distances of the particles based on their diameters and electrophoretic mobilities (Table 1). Figure 4 shows the movement of particles having similar electrophoretic mobilities but different diameters of 3.1 μm and 9.9 μm. There was no significant difference in the repulsion distances between particles. As mentioned before, the dielectrophoretic velocity of the particle is proportional to the square of the diameter. Thus, the result indicates that the dielectrophoretic force was too weak, compared with the hydrodynamic drag and electrophoretic forces, to deflect the particles.

Table 1 | Electrophoretic mobilities depending on particle diameter

particle diameter (μm)	electrophoretic mobility (10^{-4} $cm^2V^{-1}s^{-1}$)
0.05	−4.30
0.1	−4.78
0.5	−7.05
1.0	−8.60
1.1	−6.50
3.1	−6.70
4.8	−4.35
9.9	−6.18

The mobilities of particles diluted in 1-mM DSP solution were measured by a zeta potential analyzer (Zetasizer Nano Z, Malvern).

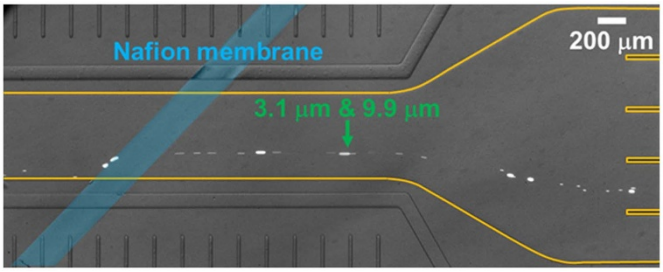

Figure 4 | Movement of particles having similar electrophoretic mobilities and different sizes; diameters: 3.1 and 9.9 μm; electrophoretic mobilities: -6.70×10^{-4} and -6.18×10^{-4} $cm^2 \cdot V^{-1} \cdot s^{-1}$, respectively (snap shot; flow rate of Inlet 1: 1.0 μL/min; flow rate of Inlet 2: 50 nL/min; applied voltage: 60 V, membrane thickness: 1.3 μm).

Figure 5a shows the separation of particles having similar diameters but different electrophoretic mobilities; 1.0-μm particles had a higher electrophoretic mobility than 1.1-μm particles (see the Supplementary Video 1). After the particles passed over a Nafion membrane, the trajectory of the 1.0-μm particles deviated more than that of the 1.1-μm particles. To quantitatively analyze the effect of electrophoresis, we measured the repulsion distance of particles having different mobilities using one device under fixed experimental conditions. There was a positive correlation between repulsion distance and electrophoretic mobility, regardless of particle diameter (Figure 5b). This result supports the hypothesis that the electrophoretic force was the dominant repulsive force in the depletion region.

Separation of micro- and nano-sized particles. Electrophoresis in the depletion region can be applied to separate a wide range of particle sizes, from the nanoscale to the microscale. Figure 6a shows the separation of microparticles having different electrophoretic mobilities (see the Supplementary Video 2). The 9.9-μm particles experienced greater deflection from the fluid flow, due to their higher electrophoretic mobility, compared to the 4.8-μm particles; thus, the two particle sizes were separated. Nanoparticles of 100 nm and 500 nm were separated in the same manner (Figure 6b, see the Supplementary Video 3). Similar to the separation of micro-sized particles, 500-nm particles, having higher electrophoretic mobility, were deflected more than 100-nm particles. The two particle sizes were separated, but the dispersion of the nanoparticles was greater than that of microparticles.

Particle dispersion is a limitation of the ICP-based separation device. Because the membrane was patterned only on the bottom of the separation channel, the repulsive force applied to the particles depended on the distance of the particles from the membrane as well as from the lower side wall. To reduce dispersion and improve the separation resolution, three-dimensional flow focusing will be adapted to the device. By focusing particles on the bottom surface of the separation channel, an identical force will be applied to particles having the same diameter. Meanwhile, the loss of electrical potential occurred in the separation and buffer channels due to the long distance between the electrodes (about 1.2 cm). However, because most of the potential drop occurred in the depletion region due to the nature of ICP[21], the loss was negligible.

Discussion

When voltage is applied to the separation device, the electric field must pass through the Nafion membrane from the separation channel into the buffer channel, thus the electric field takes a turn towards the lower side wall at the depletion region along the membrane. As a

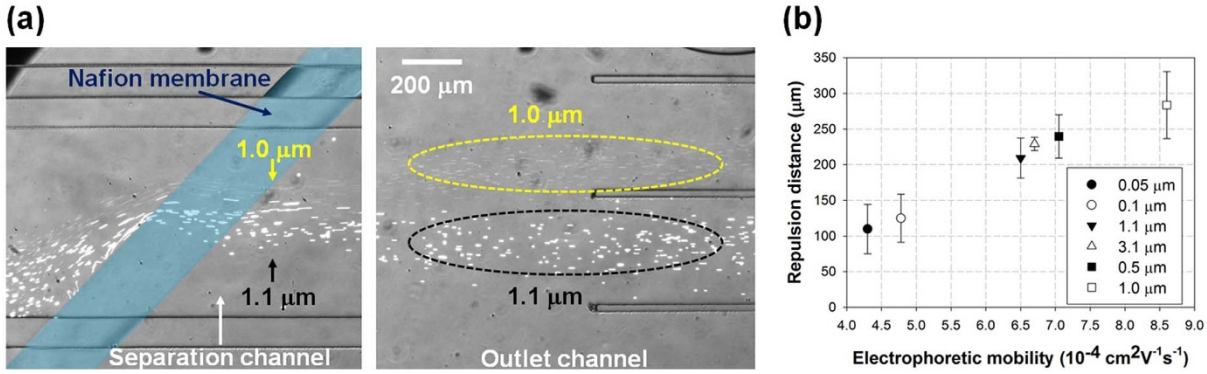

Figure 5 | Analysis of electrophoretic force in the depletion region. (a) Separation of particles having similar diameters and different electrophoretic mobilities; diameters: 1.0 and 1.1 μm and electrophoretic mobilities: -8.56×10^{-4} and -6.42×10^{-4} $cm^2 \cdot V^{-1} \cdot s^{-1}$ (snap shot; flow rate of Inlet 1: 0.5 μL/min; flow rate of Inlet 2: 30 nL/min; applied voltage: 53 V; membrane thickness: 5 μm). (b) Change in the repulsion distance depending on the absolute value of electrophoretic mobility (error bars represent the range of particle dispersion; flow rate of Inlet 1: 0.5 μL/min; flow rate of Inlet 2: 30 nL/min; applied voltage: 50 V; membrane thickness: 5 μm).

result, the electric field in the depletion region would have normal component to the flow. Therefore, when negatively charged particles were injected into the depletion region by fluidic stream, they were deflected in the normal direction to the stream by the electrophoretic force. The shifted distance from the stream was determined by electrophoretic mobility of the particles, so the separation was achieved.

To separate particles in such limited area (the depletion region), strong electric field must be applied to particles inside the region. Recent one-dimensional modeling studies demonstrated that the electric field in the depletion region can be amplified 20 times over than external field because of the low ionic concentration[21,25,26]. Therefore, although the external electric field of 50 V/cm (50–70 V in about 1.2 cm long distance between electrodes) was applied, strong electric field (up to 1000 V/cm) can be formed for separating particles in the depletion region.

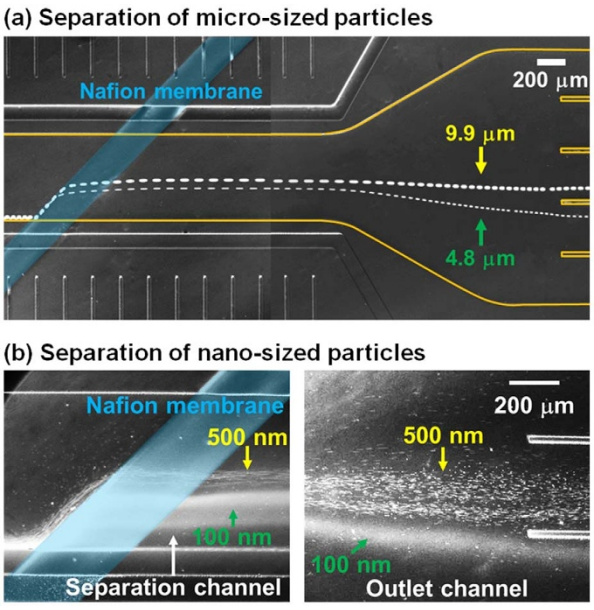

Figure 6 | Separation of micro- and nano-sized particles depending on electrophoretic mobility. (a) Diameters: 4.8 and 9.9 μm, electrophoretic mobilities: -4.35×10^{-4} and -6.18×10^{-4} $cm^2 \cdot V^{-1} \cdot s^{-1}$ (trajectories of each particle; flow rate of Inlet 1: 1.0 μL/min; flow rate of Inlet 2: 50 nL/min; applied voltage: 66 V; membrane thickness: 1.3 μm). (b) Diameters: 100 and 500 nm; electrophoretic mobilities: -4.76×10^{-4} and -7.25×10^{-4} $cm^2 \cdot V^{-1} \cdot s^{-1}$ (snap shot with high contrast to distinguish particles; flow rate of Inlet 1: 0.5 μL/min; flow rate of Inlet 2: 30 nL/min; applied voltage: 63 V; membrane thickness: 5 μm).

We experimentally verified that the dielectrophoretic force was negligible in the depletion region, compared with hydrodynamic drag and electrophoretic forces. The weak dielectrophoretic force indicated that the electric field gradient was also weak in the depletion region. However, the electric field distribution can vary depending on the channel structure, membrane material and structure and buffer solution. Therefore, in specific experimental conditions, the intensity of the dielectrophoretic force can be sufficient to affect the movement of the sample. Kim *et al.* performed desalination using ICP and reported that the movement of both positively and negatively charged particles was blocked in the depletion region[19]. The blocking of positively charged particles cannot be explained by the electrophoretic force, because the direction of the force is opposite to that of negatively charged particles. We conjectured that the dielectrophoretic force was strong in the system used by Kim *et al.* and may have blocked the positively charged particles. However, this question was not intensively studied, and additional research is needed for verification.

The rapid decrease of ion concentration in the depletion region can develop a strong gradient of ion concentration. Due to the strong concentration gradient, diffusiophoresis may affect the motion of particles[27,28]. Unfortunately, because it is hard to control the concentration gradient experimentally, we could not perform experiments to examine the effects of diffusiophoresis. Instead, theoretical and numerical analyses were carried out for evaluating the effects of diffusiophoresis in the depletion region (see the Supplementary Note). Because the analyses showed that the diffusiophoretic force was significantly weaker compared to the electrophoretic force in the depletion region, we neglected the diffusiophoretic force.

In summary, we developed a novel continuous electrophoretic separation method using ICP. Experiments were performed to verify the principles and investigate the characteristics of this method. The electrical repulsion generated in the depletion region was used to separate samples. Experiments demonstrated that electrophoresis was the dominant repulsion mechanism, so the separation was achieved depending on not size but electrophoretic mobility. This separation device is applicable to the separation of nanoparticles as well as microparticles. Due to the characteristic of electric field having normal component in the depletion region of ICP, the separation can be performed with external electrodes. The absence of internal electrodes allows this method to offer advantages of simple, low-cost device fabrication and bubble-free operation, which makes the integration with other elements of μ-TAS easy. Also, separation of samples can be achieved even under low voltages, and retention time was

short (less than a few seconds) because samples can be separated in the confined depletion region, where the electric field is strongly amplified. Due to the short retention time, sample aggregation[29] and Brownian diffusion which decreases separation efficiency could be minimized. Furthermore, by combining this method with the ICP-based concentrator[3,16], it is possible to increase the separation efficiency and detection sensitivity. Although the issue of dispersion remains a challenge, we expect that this separation device will be a useful tool for separating various biochemical samples, including cells[30,31], proteins, DNAs[32,33] and ions. In addition, this research offers insight into the origin of the electrical repulsion in the depletion region formed by ICP.

Methods

Device fabrication. We fabricated a polydimethylsiloxane (PDMS) microfluidic device using conventional photolithography (microchannel height: 40 μm)[34]. As shown in Figure 1, two microchannels, separation and buffer channels, were connected by a Nafion membrane (nanojunction) with strong cation selectivity[3]. The Nafion membrane was patterned on a glass substrate using a Nafion perfluorinated ion-exchange resin (20 wt%; Sigma-Aldrich) via the microflow patterning method[35]. To reduce the flow instability caused by the vortex in the depletion region, the Nafion membrane was inclined at an angle of 45° (Figure 1)[3,16,36]. A thicker membrane generates a stronger electrical repulsive force around the membrane[37]. However, when the membrane is thicker than 3 μm, particles with diameters larger than 4.8 μm can become trapped in the edge of the membrane. Therefore, when those large particles were included in the sample, we used the membrane with a thickness of about 1.3 μm; for the other samples, we used the membrane with a thickness of about 5 μm. The plasma-treated PDMS microfluidic layer was bonded to the Nafion-patterned glass substrate to connect the separation and buffer channels through the Nafion membrane. To amplify the separation distance between particles, the outlet width was expanded by three times compared with the separation channel (separation channel width: 600 μm; broadened outlet width: 1800 μm).

Materials and procedure for separation. In experiments, we used fluorescent polystyrene particles (Thermo scientific Corp. and Invitrogen) with various sizes and electrophoretic mobilities, but all of the mobilities have negative sign (see the Table 1). 1-mM dibasic sodium phosphate (DSP) was used as a buffer solution. An electric field was applied to the separation device by using a function generator (33220A, Agilent) and an amplifier (A800, FLC Electronics). The flow rates of Inlet 1 and 2 were regulated by using two syringe pumps (Pump 11 Elite, Harvard Corp.). An inverted fluorescent microscope (Axiovert 200, Carl zeiss) and a CCD camera (Sensicam qe, PCO) were used to observe the trajectories of the fluorescent particles and collect images from the device.

To apply an electric field to the device, anode and cathode electrodes were connected to the metallic syringe tube of Inlet 1 and reservoir of the buffer channel, respectively. The electric field applied across the membrane induced an ion-depletion region (red circle in Figure 1) on the anodic side due to its strong cation selectivity[3]. A flow-focusing method[22] was used to drive the particles to the lower side wall of the separation channel, causing the particles to pass through the depletion region, where the electrical force was strong.

1. Turgeon, R. T. & Bowser, M. T. Micro free-flow electrophoresis: theory and applications. *Anal. Bioanal. Chem.* **394**, 187–198 (2009).
2. Pamme, N. Continuous flow separations in microfluidic devices. *Lab Chip* **7**, 1644–1659 (2007).
3. Kwak, R., Kim, S. J. & Han, J. Continuous-flow biomolecule and cell concentrator by ion concentration polarization. *Anal. Chem.* **83**, 7348–7355 (2011).
4. Kohlheyer, D., Besselink, G. A. J., Schlautmann, S. & Schasfoort, R. B. M. Free-flow zone electrophoresis and isoelectric focusing using a microfabricated glass device with ion permeable membranes. *Lab Chip* **6**, 374–380 (2006).
5. Becker, M., Marggraf, U. & Janasek, D. Separation of proteins using a novel two-depth miniaturized free-flow electrophoresis device with multiple outlet fractionation channels. *J. Chromatogr. A* **1216**, 8265–8269 (2009).
6. Frost, N. W. & Bowser, M. T. Using buffer additives to improve analyte stream stability in micro free flow electrophoresis. *Lab Chip* **10**, 1231–1236 (2010).
7. Köhler, S., Nagl, S., Fritzsche, S. & Belder, D. Label-free real-time imaging in microchip free-flow electrophoresis applying high speed deep UV fluorescence scanning. *Lab Chip* **12**, 458–463 (2012).
8. Kostal, V., Fonslow, B. R., Arriaga, E. A. & Bowser, M. T. Fast determination of mitochondria electrophoretic mobility using micro free-flow electrophoresis. *Anal. Chem.* **81**, 9267–9273 (2009).
9. Kohlheyer, D., Eijkel, J. C. T., Van den Berg, A. & Schasfoort, R. B. M. Miniaturizing free-flow electrophoresis - a critical review. *Electrophoresis* **29**, 977–993 (2008).
10. Zhang, C.-X. & Manz, A. High-speed free-flow electrophoresis on chip. *Anal. Chem.* **75**, 5759–5766 (2003).
11. Podszun, S. *et al.* Enrichment of viable bacteria in a micro-volume by free-flow electrophoresis. *Lab Chip* **12**, 451–457 (2012).
12. Janasek, D., Schilling, M., Manz, A. & Franzke, J. Electrostatic induction of the electric field into free-flow electrophoresis devices. *Lab Chip* **6**, 710–713 (2006).
13. Kim, S. J., Wang, Y.-C., Lee, J. H., Jang, H. & Han, J. Concentration polarization and nonlinear electrokinetic flow near a nanofluidic channel. *Phys. Rev. Lett.* **99**, 044501 (2007).
14. Yossifon, G. & Chang, H.-C. Selection of nonequilibrium overlimiting currents: universal depletion layer formation dynamics and vortex instability. *Phys. Rev. Lett.* **101**, 254501 (2008).
15. Kim, P., Kim, S. J., Han, J. & Suh, K. Y. Stabilization of ion concentration polarization using a heterogeneous nanoporous junction. *Nano lett.* **10**, 16–23 (2010).
16. Kim, S. J., Song, Y.-A. & Han, J. Nanofluidic concentration devices for biomolecules utilizing ion concentration polarization: theory, fabrication, and applications. *Chem. Soc. Rev.* **39**, 912–922 (2010).
17. Pu, Q., Yun, J., Temkin, H. & Liu, S. Ion-enrichment and ion-depletion effect of nanochannel structures. *Nano Lett.* **4**, 1099–1103 (2004).
18. Zangle, T. A., Mani, A. & Santiago, J. G. Theory and experiments of concentration polarization and ion focusing at microchannel and nanochannel interfaces. *Chem. Soc. Rev.* **39**, 1014–1035 (2010).
19. Kim, S. J., Ko, S. H., Kang, K. H. & Han, J. Direct seawater desalination by ion concentration polarization. *Nat. Nanotechnol.* **5**, 297–301 (2010).
20. Kim, D., Raj, A., Zhu, L., Masel, R. I. & Shannon, M. A. Non-equilibrium electrokinetic micro/nano fluidic mixer. *Lab Chip* **8**, 625–628 (2008).
21. Kim, S. J., Li, L. D. & Han, J. Amplified electrokinetic response by concentration polarization near nanofluidic channel. *Langmuir* **25**, 7759–7765 (2009).
22. Garstecki, P., Stone, H. A. & Whitesides, G. M. Mechanism for flow-rate controlled breakup in confined geometries: a route to monodisperse emulsions. *Phys. Rev. Lett.* **94**, 164501 (2005).
23. Devasenathipathy, S., Santiago, J. G. & Takehara, K. Particle tracking techniques for electrokinetic microchannel flows. *Anal. Chem.* **74**, 3704–3713 (2002).
24. Kang, K. H., Xuan, X., Kang, Y. & Li, D. Effects of dc-dielectrophoretic force on particle trajectories in microchannels. *J. Appl. Phys.* **99**, 064702 (2006).
25. Dhopeshwarkar, R., Crooks, R. M., Hlushkou, D. & Tallarek, U. Transient effects on microchannel electrokinetic filtering with an ion-permselective membrane. *Anal. Chem.* **80**, 1039–1048 (2008).
26. Jin, X., Joseph, S., Gatimu, E. N., Bohn, P. W. & Aluru, N. R. Induced electrokinetic transport in micro-nanofluidic interconnect devices. *Langmuir* **23**, 13209–13222 (2007).
27. Prieve, D. C., Anderson, J. L., Ebel, J. P. & Lowell, M. E. Motion of a particle generated by chemical gradients. part 2. electrolytes. *J. Fluid Mech.* **148**, 247–269 (1984).
28. Rica, R. A. & Bazant, M. Z. Electrodiffusiophoresis: particle motion in electrolytes under direct current. *Phys. Fluids* **22**, 112109 (2010).
29. Mitnik, L., Heller, C., Prost, J. & Viovy, J. L. Segregation in DNA solutions induced by electric fields. *Science* **267**, 219–222 (1995).
30. Krivánková, L. & Bocek, P. Continuous free-flow electrophoresis. *Electrophoresis* **19**, 1064–1074 (1998).
31. Weber, G., Grimm, D. & Bauer, J. Application of binary buffer systems to free flow cell electrophoresis. *Electrophoresis* **21**, 325–328 (2000).
32. Heller, C. Principles of DNA separation with capillary electrophoresis. *Electrophoresis* **22**, 629–643 (2001).
33. Lau, H. W. & Archer, L. A. Electrophoresis of end-labeled DNA: theory and experiment. *Phys. Rev. E* **81**, 031918 (2010).
34. Duffy, D. C., McDonald, J. C., Schueller, O. J. A. & Whitesides, G. M. Rapid prototyping of microfluidic systems in poly(dimethylsiloxane). *Anal. Chem.* **70**, 4974–4984 (1998).
35. Lee, J. H., Song, Y.-A. & Han, J. Multiplexed proteomic sample preconcentration device using surface-patterned ion-selective membrane. *Lab Chip* **8**, 596–601 (2008).
36. Rubinstein, S. M. *et al.* Direct observation of a nonequilibrium electro-osmotic instability. *Phys. Rev. Lett.* **101**, 236101 (2008).
37. Ko, S. H. *et al.* Nanofluidic preconcentration device in a straight microchannel using ion concentration polarization. *Lab Chip* **12**, 4472–4482 (2012).

Acknowledgments

This work was supported by the National Research Foundation of Korea (NRF) grant funded by the Korea government (MEST) (Grant No. 2012R1A2A2A06047424). We gratefully appreciate Dr. S.H.Ko's contribution to the original conception of this technique and helpful comments. We are grateful to S.K.Hong for the English correction of the manuscript.

Author contributions

H.J. designed and carried out experiments. H.J. and H.L. analyzed the data and wrote this manuscript. K.H.K. and G.L. supervised the research. All authors discussed the results and commented on the manuscript.

Additional information

Supplementary information accompanies this paper at http://www.nature.com/scientificreports

Competing financial interests: The authors declare no competing financial interests.

How to cite this article: Jeon, H., Lee, H., Kang, K.H. & Lim, G. Ion concentration polarization-based continuous separation device using electrical repulsion in the depletion region. *Sci. Rep.* **3**, 3483; DOI:10.1038/srep03483 (2013).

SCIENTIFIC REPORTS

DOI: 10.1038/srep06668

SUBJECT AREAS:
MICROFLUIDICS
MECHANICAL ENGINEERING

CORRIGENDUM: Ion concentration polarization-based continuous separation device using electrical repulsion in the depletion region

Hyungkook Jeon, Horim Lee, Kwan Hyoung Kang & Geunbae Lim

SCIENTIFIC REPORTS:
3 : 3483
DOI: 10.1038/srep03483
(2013)

Published:
19 December 2013

Updated:
31 October 2014

The original version of this Article contained a typographical error in the Results section.
Under the subheading 'Theoretical analysis of electrical forces', "and ζ_p and $\mathbf{u_p}$ are the dynamic viscosity and particle velocity, respectively" should read "and ζ_p and $\mathbf{u_p}$ are the surface potential and the velocity of the particle, respectively".